CHAPTER III

ELASTICITY AND ORIENTATIONAL ORDER IN SOME 4'-n-ALKYL-4-CYANOBIPHENYLS

The elastic constants of nematic liquid crystals are sensitive to the degree of order - both long range and short range - in the medium. For simple nematics wherein short range order is expected to be independent of temperature the mean field theory predicts $k_{ii} \propto S^2$. But in those compounds in which the short range order is a function of temperature, k_{ii} deviate strongly from the S^2 law.

In a homologous series of compounds various physical properties of the nematic phase alternate as the series is ascended because of the differences in the configuration of the end chain. *If* the molecules have alkyl end groups the final C-C bond in the even members of the series makes, an the average, a large angle with *the* long axis of the molecule (figure 3.1) thus reducing the molecular anisotropy. (This is strictly true for an all-trans conformation of the end chains.) On the other hand, in the odd members the final segment is nearly parallel to the long axis on the average, thus enhancing the anisotropy of the molecule. It is well known that the nematic-isotropic transition

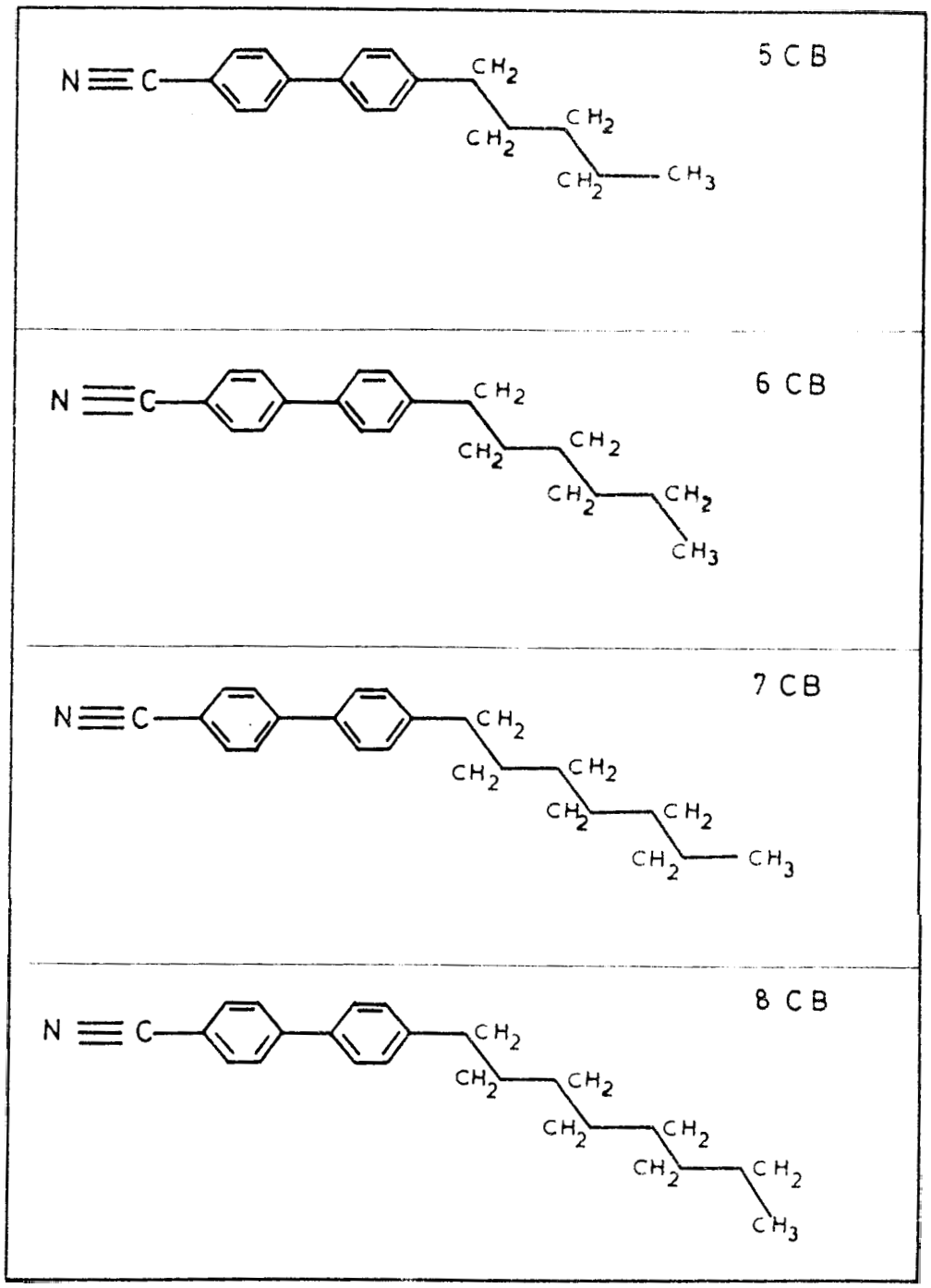

Figure 3.1

Chemical structures of 5CB, 6CB, 7CB and 8CB with the end chains in an all-trans configuration.

points (T_{NI}) and the corresponding entropy changes alternate between even and odd members of the series. This is commonly referred to as odd-even effect (see for example, Barrall and Johnson 1974). The early NMR studies of Lippman and Weber (1957) on 4,4'-n-dialkoxyazoxybenzenes clearly indicated an alternation in the values of order parameter (S_{NI}) at T_{NI}. This result has been confirmed by a more recent study (Pines et al. 1975). A detailed statistical thermodynamic treatment of the effect of end-chain conformations on the properties of the nematic phase has been given by Marcelja (1974). In particular, he has calculated the alternation of T_{NI}, ΔH and S. If the mean field theory is valid, en alternation in k_{ii} ($\propto S^2$) should also be observed.

X-ray studies on some nematics have revealed the presence of positional short range order in groups of molecules with the molecular centres in each group arranged in *layers*. These groups are called cybotactic groups. The cybotactic nematics are sub-divided into two groups (de Vries 1973) (a) normal cybotactic nematic wherein each group has smectic A type of ordering, (b) skew cybotactic nematic in which *the* ordering in each group is smectic C typo. When cybotactic groups are present in the medium, the

variation of elastic constants with temperature may to a large extent depend on the changes in the cybotactic groups.

The only systematic study of elastic constants in a homologous series to have been carried out previously is that due to Gruler (1973) on 4,4'-di-n-alkoxyazoxybenzenes. He measured only the splay and bend constants and observed that both k_{11} and k_{33} exhibit the odd-even effect near T_{NI}. Moreover the reduced splay constant

$$C_{ii} = \frac{k_{ii} V^{7/3}}{S^2}$$

(where V is the molar volume) is temperature dependent for all members of the series, except C_{11} of the first two. Further, the ratio k_{33}/k_{11} is temperature dependent PoP all the members. He correctly attributed thia to the building up *of* the positional short range order in the nematic phase as the length of end chain Pa increased. The fifth member for which the cybotactic groups begin to form, shows an anomalous decrease and then an increase in the ratio k_{33}/k_{11} as the temperature is decreased. In 4,4'-di-(n-heptyloxy) azobenzene which shows smectic C at lower temperatures he found evidence for the divergence of k_{33}/k_{11} as the

smectic-nematic transition is approached. Cheung and Meyer (1973) observed a pretransitional increase in the bend constant of p-butoxybenzylidene-p'-β-methyl butyl aniline which exhibits first order smectic A-nematic transition as T_c^* is approached. In the presence of smectic C type of short range order all the elastic constants are expected to show pretransitional increases, since the corresponding deformatione tend to alter the layer thickness (Gruler 1973). In the presence of smectic A type of short range order only bend and twist become difficult, so that only these two constants diverge. We shall discuss this aspect in detail in Chapter V.

We have undertaken a otudy of the elastic constants of two homologous series which exhibit normal cybotactic groups i.e., smectic A type of short range order.

In this Chapter we shall discuss the results of our measurements on all the elastic constants and order parameters *of* four members *of* 4'-n-alkyl-4-cyanobiphenyls (figure 3.1).

Order parameter and density

We have calculated the temperature variation of the relative order parameter and density on the

basis of optical measurements. The principal refractive indices of all the compounds were determined by the prism method (Pellet and Chatelain 1950, Madhusudana et al. 1971). Since the order parameter and density measurements are not the main theme of this thesis, we have given all the experimental details and derivations of relevant equations in Appendix XI. Ye shall present only tho experimental data in this Chapter. The expressions used for S and ρ are (see equations 7 and 8 of Appendix Xi)

$$S = \frac{\bar{\alpha}}{\Delta\alpha} \cdot \frac{n_e^2 - n_o^2}{\bar{n}^2 - 1}$$

$$\rho = \frac{3}{4\pi} \cdot \frac{M}{N} \cdot \frac{1}{\bar{\alpha}} \frac{\bar{n}^2 - 1}{\bar{n}^2 + 2} \qquad (3.1)$$

where $\bar{\alpha} = \frac{1}{3}(2\alpha_\perp + \alpha_\parallel)$ is the average polarizability of the molecule, $\Delta\alpha = \alpha_\parallel - \alpha_\perp$, $\bar{n} = \frac{1}{3}(2n_o^2 + n_e^2)$ M is the molecular weight and N is the Avogadro number.

Experimental

In Chapter X I we have already described the method of measuring the twist constant. For bend constant measurements, the same oven was used. In this case, however, the light beam was allowed to

fall normally on a homeotropically aligned sample. The sample holder is shown in figure 3.2a.

For the homeotropic alignment of tho sample, surfactants were used. In moat of the cases, the clean glass plater were dipped in a dilute aqueous solution of a cleaning agent, viz., Teepol (BDH India Ltd.)(2 drops in 2 ml of water) and dried so that a thin uniform layer of it is deposited on the glass plates. In some cases, the glass plates, after cleaning were dipped in a dilute solution of cetyl trimethyl ammonium bromide (CTMAB) in chloroform (~10 mgm in 2 ml). The glass plates were then rubbed circularly by filter paper so that a thin uniform layer of CTMAB is formed on the plates.

The sample was viewed through a low power microscope between crossed polarizers set at 45° to the magnetic field direction. As the deformation occurs in the sample the dark field of view becomes bright. The magnetic field at which the field of view becomes just bright la the critical field corresponding to the Freedericksz transition.

For the splay elastic constant determination, the length of the oven had to be reduced because, in this case, the magnetic field acts along the axis of

b

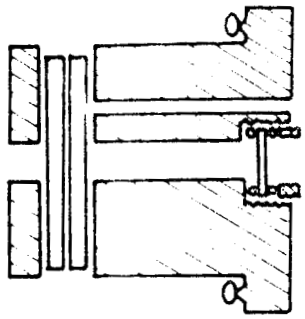

a

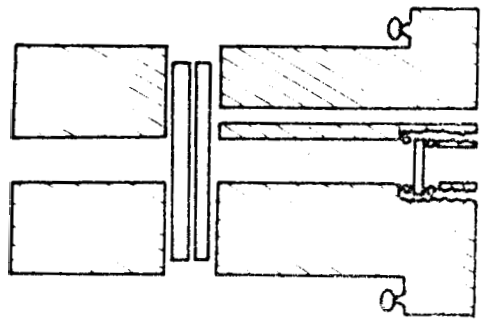

Figure 3.2

Sample holders used to study (a) k_{33} and (b) k_{11}.

the cylindrical oven. The schematic diagram of the experimental set up is shown in figure 3.3. The length sf the oven is $\sim$ 5 cm. Yet, this length is large compared to the thickness ($\sim$ 25-50 μm) of the sample. The front silvered mirror M_1 enables the collimated linearly polarized light from a sodium vapour lamp to fall on the sample normally. The emergent light which is reflected by a similar mirror M_2, passes through a quarter *wave* plate Q anti an analyser A and is observed through an eye-piece E of a low power microscope. Tho whole set up is mounted on a base provided with side screws S_1 and S_2 and levelling screws L_1, L_2 and L_3 as before. The sample holder is shown in figure 3.2b.

Initially the polarizer axis is kept at 45° to $\vec{n}$. Then Q as well as A are adjusted to get a dark field of view. Since the light is reflected by front aluminised mirrors, the emergent light, even in the absence of *the* sample, is slightly elliptic (actual analysis of the light reflected by two mirrors show that light has an azimuth of $\sim$ 2° and ellipticity $\sim$ 0.1). For this reason, at different temperatures, both Q and A are to *be* adjusted to get a dark field *of* view.

A homogeneously aligned sample is obtained by

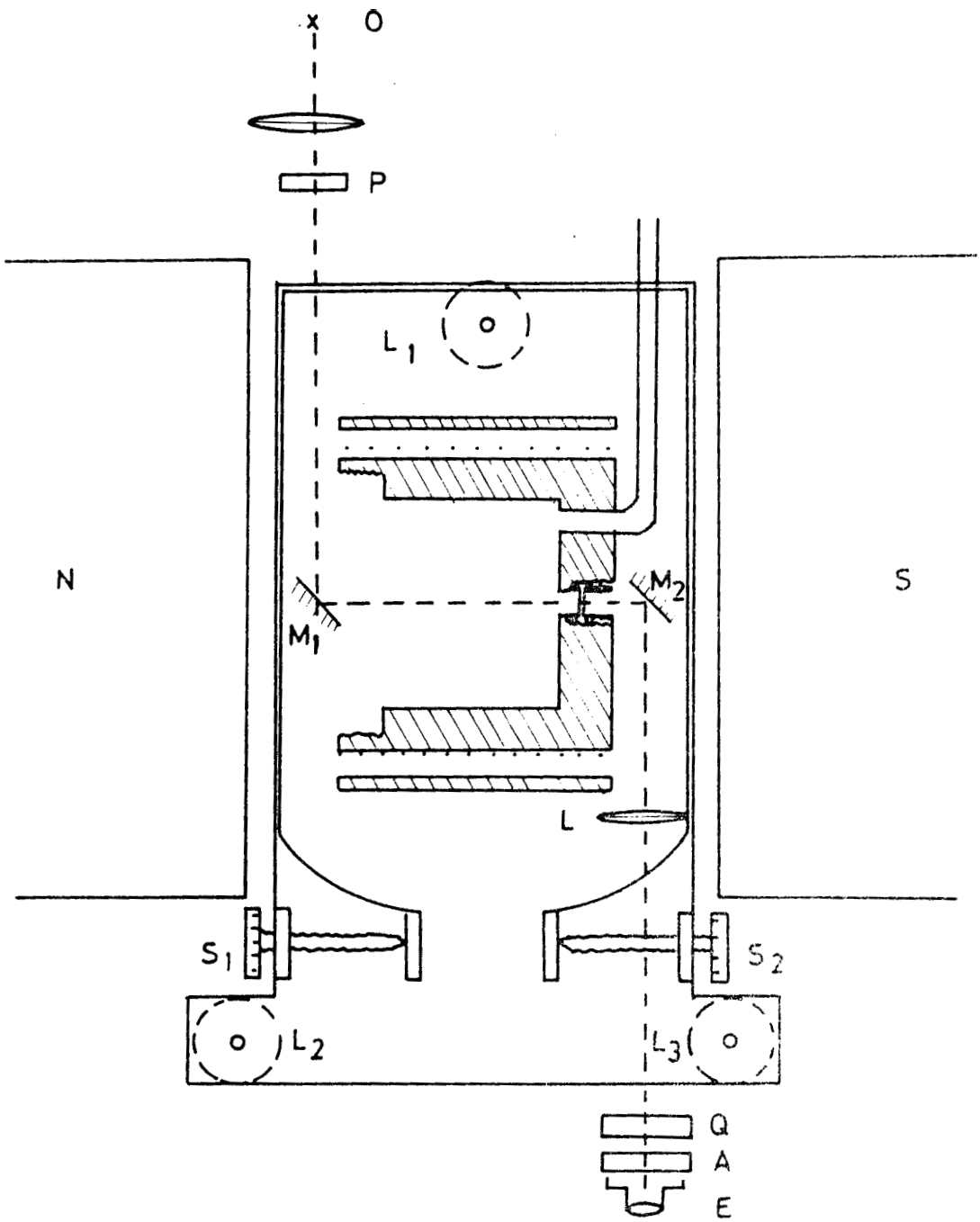

Figure 3.3

Diagram showing the set up to study k_{11}. Heater with the base is placed between tho pole pieces N and S of the electromagnet. The direction of propagation of the light beam (starting from source O) is shown by the dashed line.

rubbing the glass plates prior *to* the introduction of the sample. However, in some cases we have used the technique of vacuum deposition of silicon at an oblique angle on the glass plates (Janning 1972). Guyon et al. (1973) found that the alignment induced by the films depends on the angle of deposition. For angler between 45? and 80°, the molecules align parallel to the glass plates in a direction perpendicular to the projection on the plate, of the direction of vapour deposition.

As explained in Chapter II for a critical field to exist, the magnetic field must be exactly normal to the undistorted director. When this adjustmeat is made, as the field is increased beyond a critical value, a number of inversion walls are seen. A typical example is given in figure 3.4.

Other aspects of the experimental procedure are similar to those described in Chapter II.

Materials

We have made measurements on the fifth, sixth, seventh and eighth homologues of 4'-n-alkyl-4-cyanobiphenyl series. These *were* prepared first by Gray et al. (1973). They are exceptionally stable, colourless

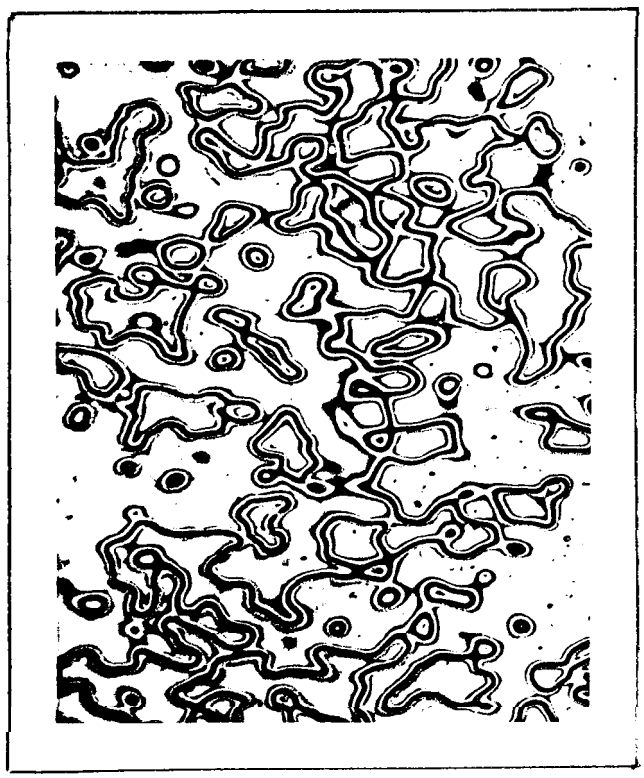

Figure 3.4

Inversion walls seen as the magnetic field is increased beyond H_c when $\vec{n}$ is exactly normal to $\vec{H}$. The sample is 7CB. The sample thickness is $\sim$ 25 μm and $H \sim 1.2\ H_c$. The photograph was taken 30 aecs. after the magnetic field was switched on.

mesogens which possess large positive dielectric anisotropy and exhibit mesophase at room temperature. For these reasons, these compounds are commonly used For twisted nematic type of display devices.

The compounds, used for our experiments, were prepared in our chemistry laboratory, adopting Gray's procedure (Gray et al. 1974). The transition temperatures and heats of nematic isotropic transitions are given in table 3.1.

Results and calculations

From Chapter I, we have tho equation

$$k_{11} = \frac{H_c^2 x_o^2}{\pi^2} \Delta\chi_{om} \cdot S \cdot \rho$$

(i) Diamagnetic susceptibility: If ΔK is tha anisotropy of the magnetic susceptibility of a gm molecule of the substance

$$\Delta\chi_{om} = \frac{\Delta K}{M}$$

where M is its molecular weight.

As before assuming that the anisotropy of susceptibility is essentially determined by the aromatic part of the molecule, ΔK is constant for all members

of the series. The measurements on biphenyl give $\Delta K = 118.6 \times 10^{-6}$ c.g.s. units (Lonsdale 1937). Assuming this value for all compounds, we have calculated the values of $\Delta\chi$ for these compounds. The values are given in Table 3.2.

(ii) Refractive indices: The values of refractive indices at various temperatures for the wavelengths λ5461 Å, λ5893 Å, λ6328 Å are given in Table 3.3. They are plotted in figure 3.5. The values from independent measurements on different samples are marked separately. The refractive index values are estimated to be accurate to ± 0.001.

(iii) Density : We have measured the density of 7CB and 5CB at room temperature (25°C) by the specific gravity bottle method (see Appendix II). Using the equation (3.1) $\bar{\alpha}_{7CB}$ and $\bar{\alpha}_{5CB}$ can be calculated for different wavelengths. To obtain the values of $\bar{\alpha}_{6CB}$ and $\bar{\alpha}_{8CB}$ we have added the value $(\frac{\bar{\alpha}_{7CB} - \bar{\alpha}_{5CB}}{2})$ to $\bar{\alpha}_{5CB}$ and $\bar{\alpha}_{7CB}$ respectively. As a cross check we calculated ρ_{6CB} at 25°C from the value of $\bar{\alpha}_{6CB}$. (For this purpose we normalised the values of $(\frac{\bar{n}^2 - 1}{\bar{n}^2 + 2})$ for λ5461 Å and λ6328 Å to that for λ5893 Å at the lowest temperature at which measurements were made. At all other temperatures, the normalised

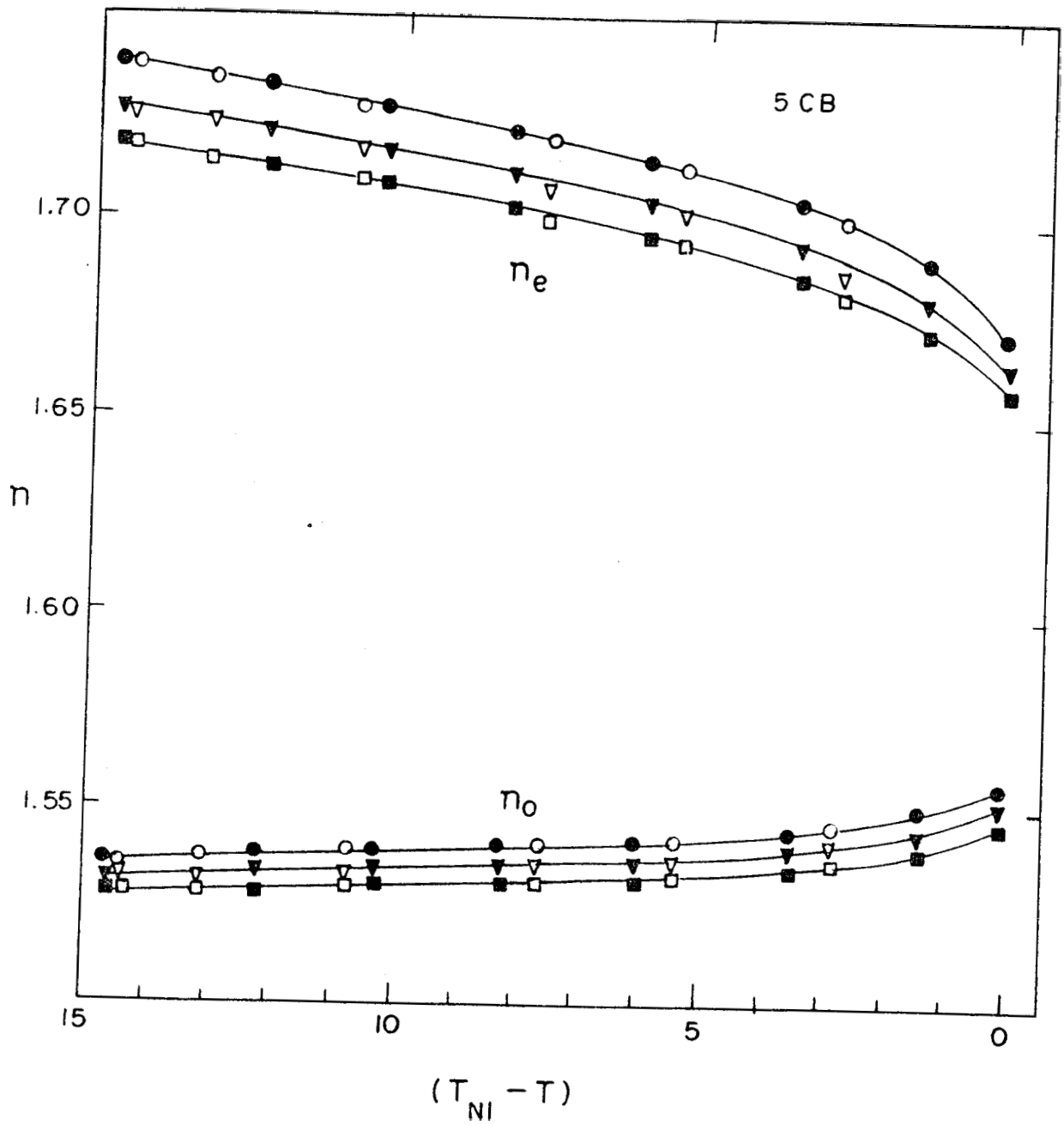

Figure 3.5a

The refractive indices of 5CB as functions of temperature. The circles, triangles and squares are the values for λ5461 A, λ5893 A and λ6328 Å respectively. Open and filled symbols represent values from independent measurements. (This holds good for all the diagrams unless stated otherwise.)

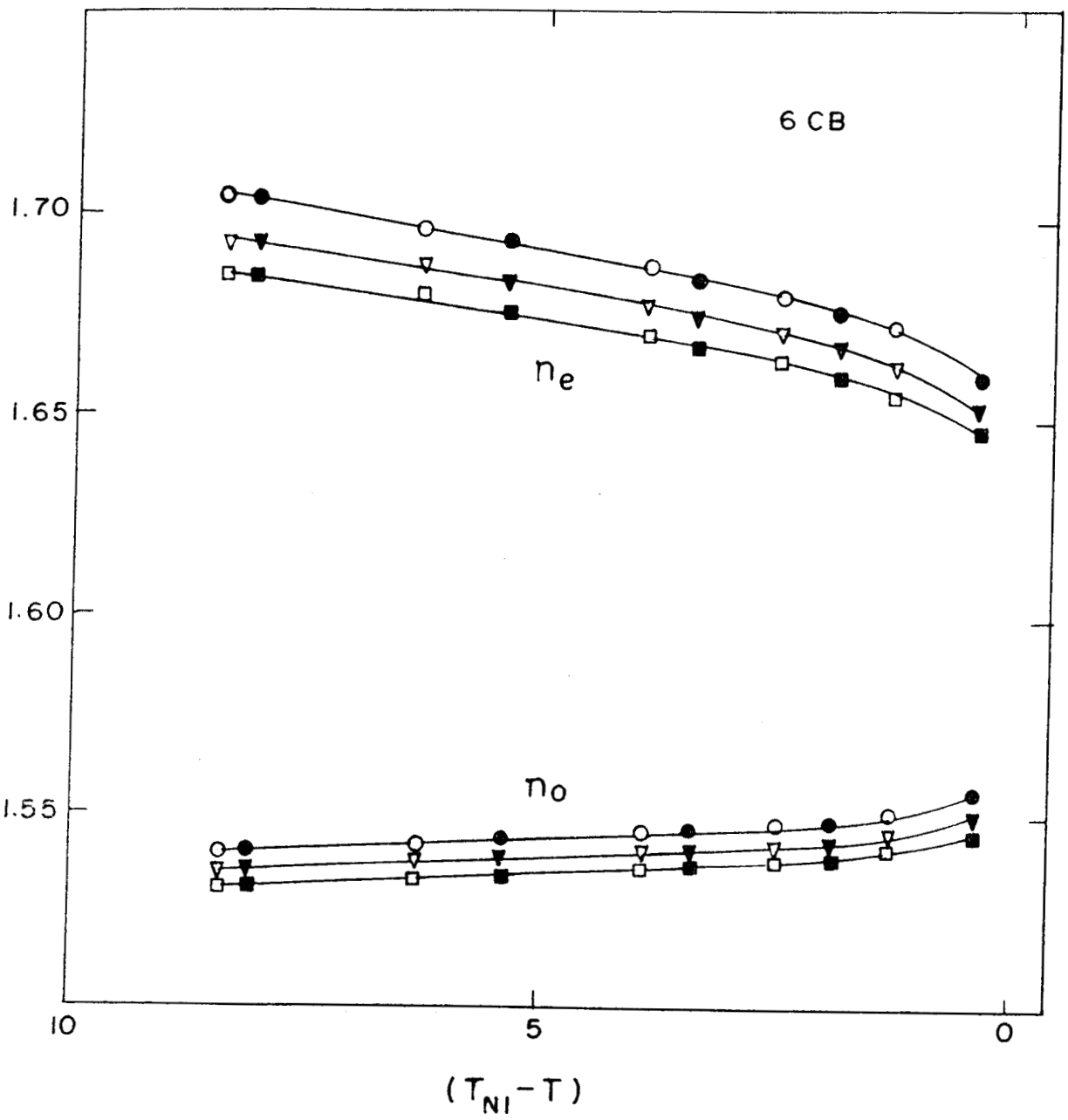

Figure 3.5b

The refractive indices of 6CB as functions of temperature. The circles, triangles and squares are the values for λ5461 Å, λ5893 Å and λ6328 Å respectively.

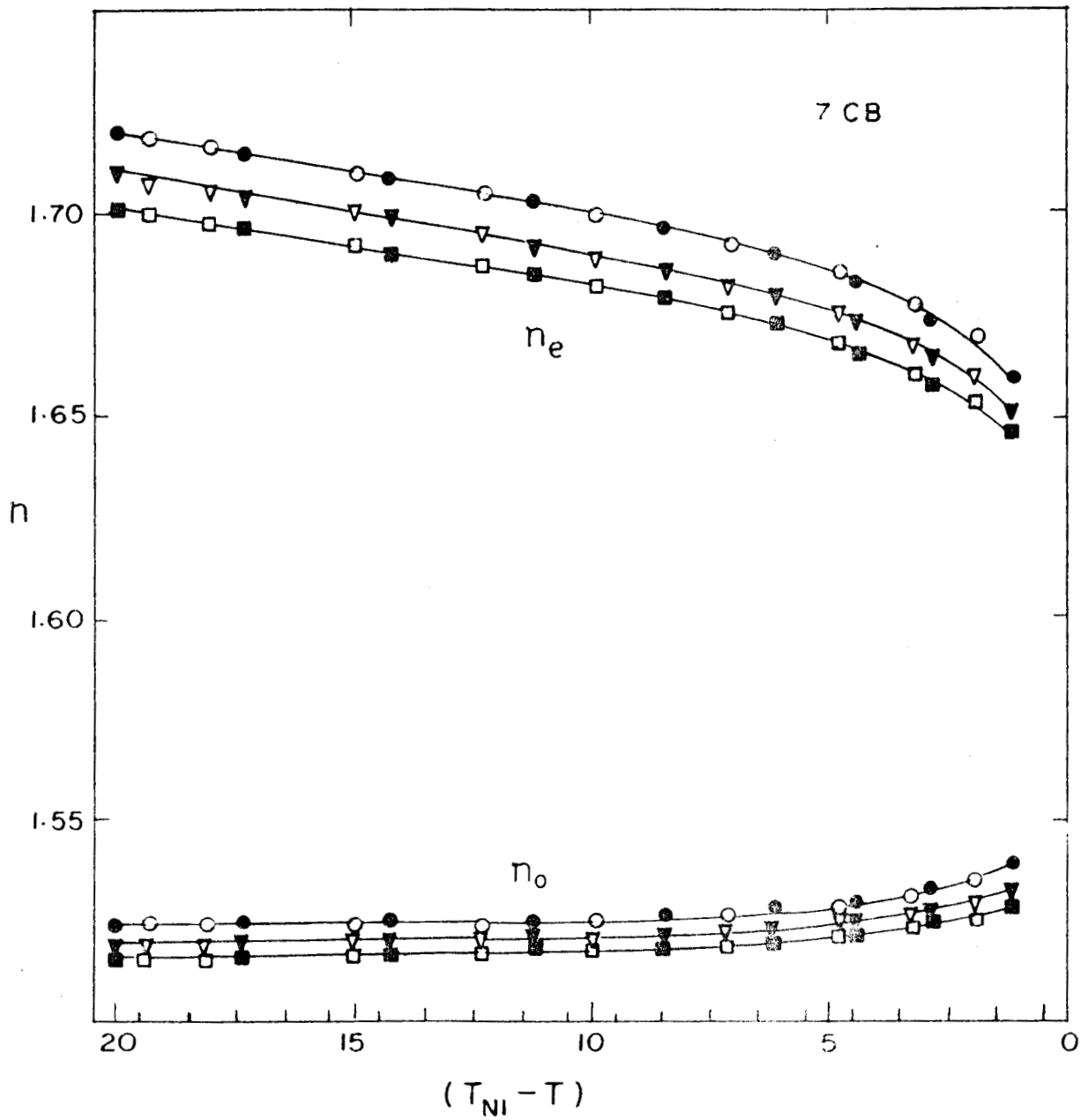

Figure 3.5c

The refractive indices *of* 7CB as functions of temperature. The circles, triangles and squares are the values for λ5461 Å, λ 5893 Å and λ6328 Å respectively.

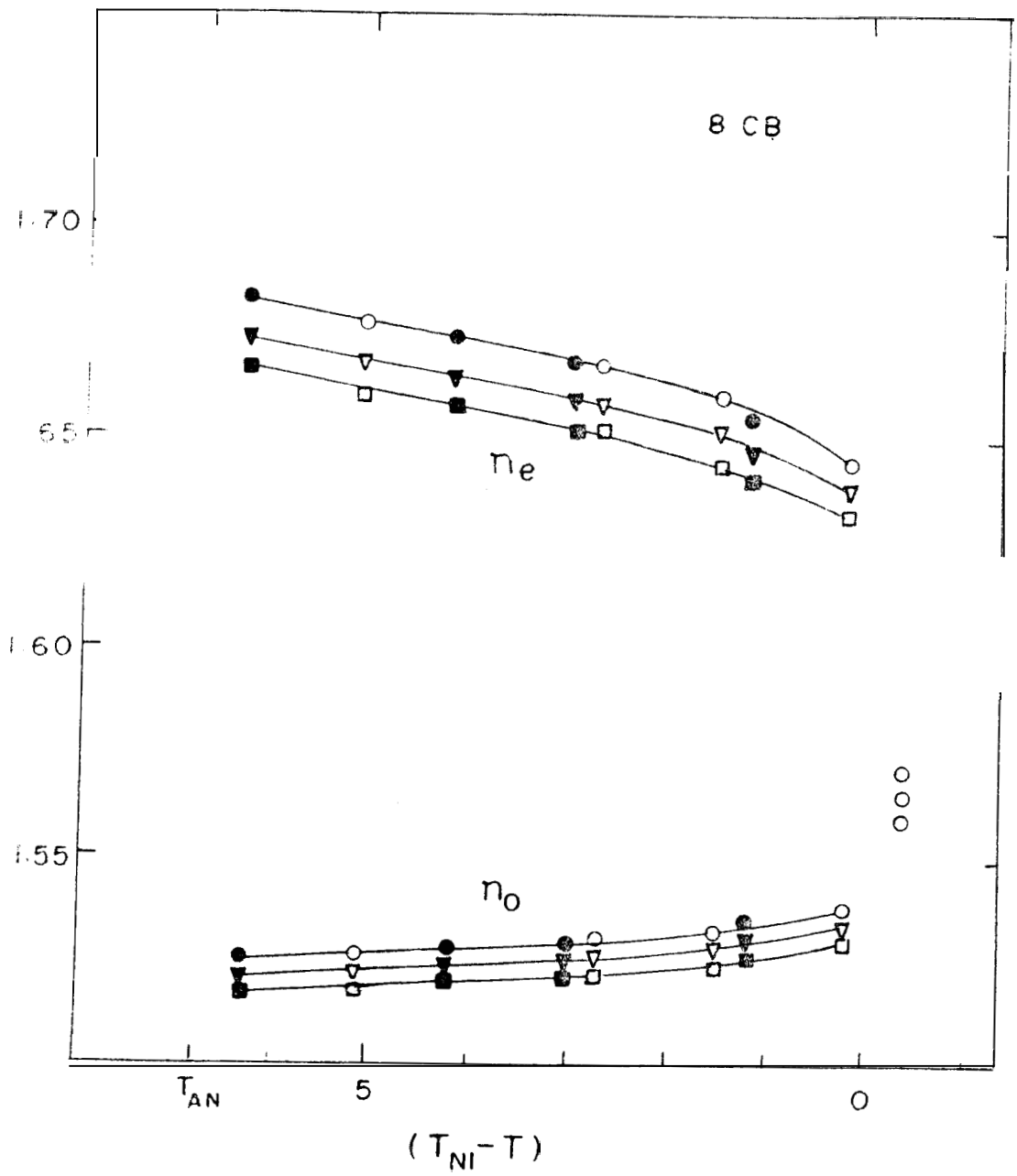

Figure 3.5d

The refractive indices of 8CB as functions of temperature. The circles, triangles and squares are the values for λ5461 Å, λ5893 Å and λ6328 Å respectively.

values for different wavelengths agree quite well. The mean of normalized $[(\overline{n^2}-1)/(\overline{n^2}+2)]$ is used to calculate ρ). The value of ρ_{6CB} calculated by this procedure agrees well with that measured by a capillary method (see Appendix II). The values of density and average polarizability $\bar{\alpha}$ are given in Table 3.4. $\bar{\alpha}$ can be expected to be independent of temperature as has been indeed observed in several compounds (Madhusudana et al. 1971, Chandrasekhar and Madhusudana, 1969). We have calculated ρ for various relative temperatures using equation (3.1). They are given in Table 3.5. This table also gives the density calculated from the data of different wavelengths. The values from independent measurements on different samples are given separately. The teapara—a variation of density is plotted in figure 3.6.

(iv) Order parameter S: There has been a recent determination of S in 7CB using Raman depolarization measurements (Heger 1975). *The* relative values of S and $[(n_e^2 - n_o^2)/(\overline{n^2} - 1)]$ [see equation (3.1)] agree quite well. For example with $\frac{\bar{\alpha}}{\Delta\alpha} = 4$ λ5893 Å, the order parameter calculated from optical anisotropy measurements agree with the reported S values to better

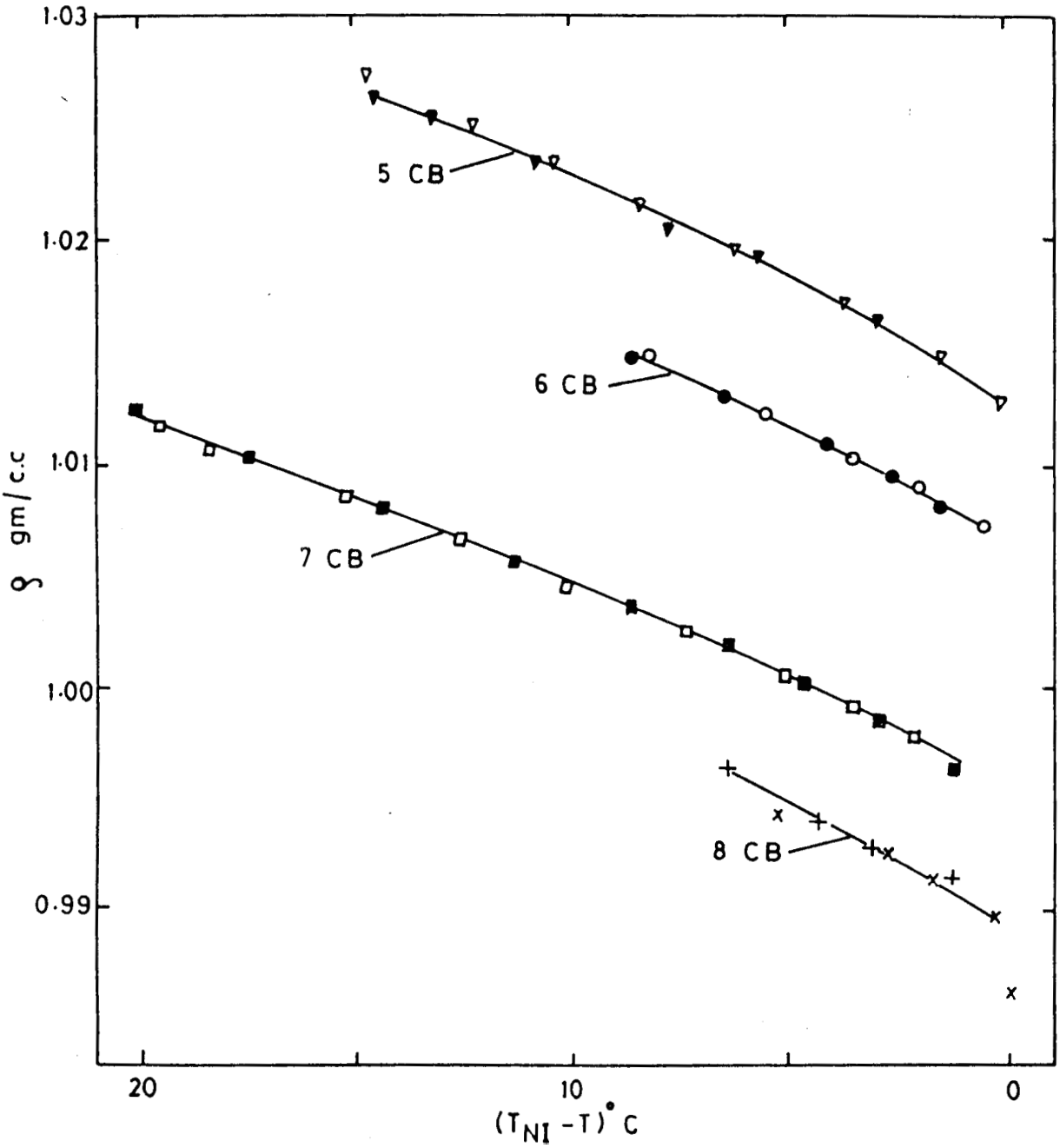

Figure 3.6

Density derived from the optioal measurements as a function of the relative temperature for 5CB-8CB. The values obtained for different samples are marked separately. Each symbol represents a value averaged over the calculations far three wavelengths.

than ±2% throughout the nematic range. Using $\bar{\alpha}$ values from density data, $\Delta\alpha_{7CB}$ can be calculated. The increment in $\Delta\alpha$ on going from one member of the series to the next higher one is estimated by using bond moments and angles of CH_2 group. The details are given in Appendix II. Here we assume that the end chain has an all-trans conformation. Although this assumption is not very good In the nematic phase, the uncertainty in S is less than 1% (e.g., an increment of +0.26 between an even to the next higher odd member of the series while $\Delta\alpha$ 30). The estimated values of $\Delta\alpha$ and $\bar{\alpha}/\Delta\alpha$ are given in Table 3.6. The absolute values of S at various temperatures can then be calculated. The temperature variation of S is given in Table 3.7. The S values from λ5461 Å and λ6328 Å are normalised to that from λ5893 Å at the lowest temperature at which the measurements were made. The values are plotted in figure 3.7. The data for different samples are marked separately.

Latent heats of transition

have used the differential scanning calorimetric measurements (Perkin-Elmer DSC-2, USA) to estimate the latent heats of transitions. The details are given in Appendix II. The nematic-isotropic transition latent

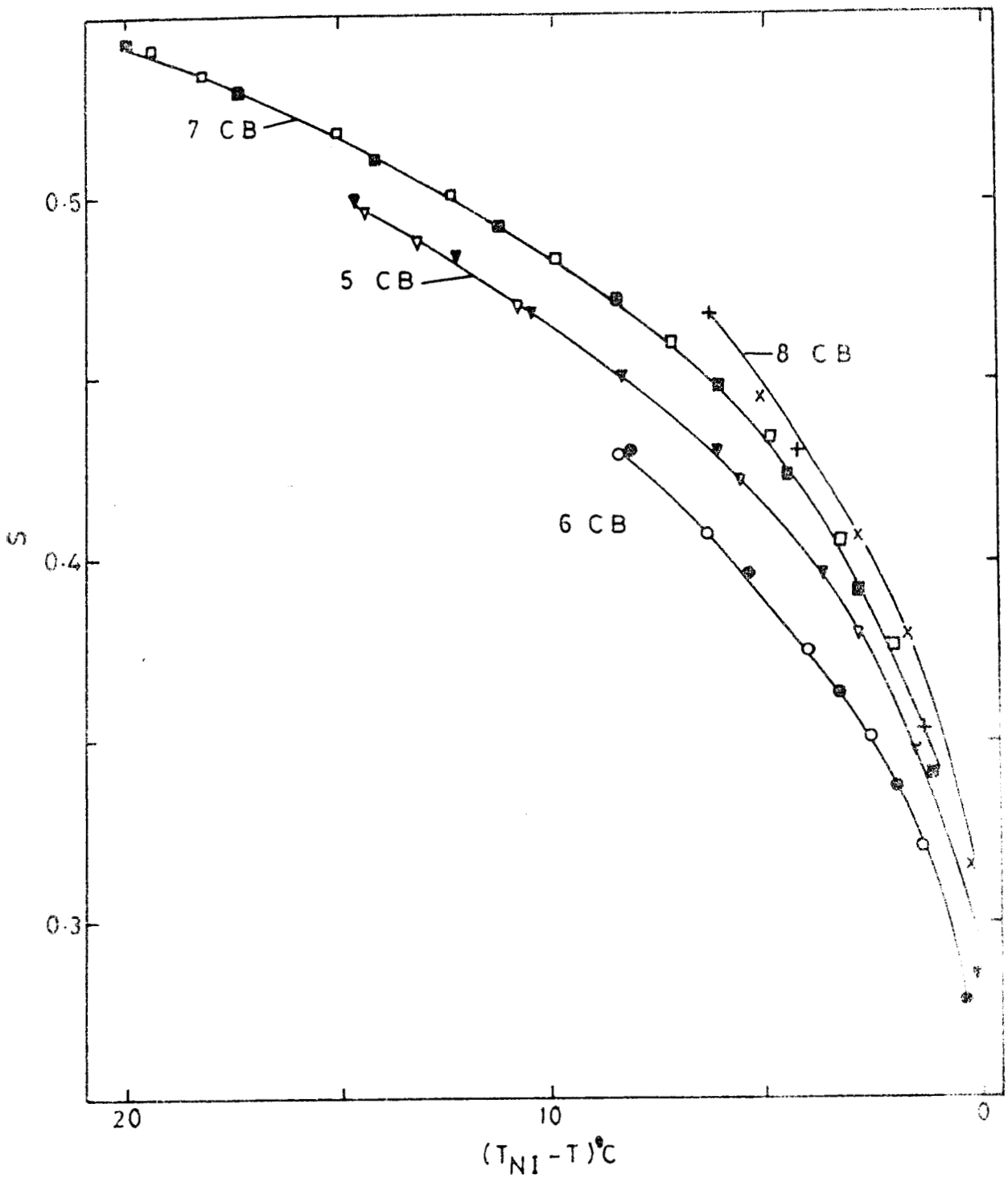

Figure 3.7

The order parameter as a function of the relative temperature for 5CB-8CB. The values for λ 5461 Å and λ 6328 Å have been normalised with that for λ 5893 Å at the lowest temperature. The averaging has been done as in figure 3.6.

heats are given in table 3.1.

Elastic constants

Using the values of $\Delta\chi_{om}$, S and ρ given above the absolute values of elastic constants have been calculated.

Tables 3.8, 3.9 and 3.10 give the splay, twist and bend constants at different temperatures. We have least square fitted the elastic constant values to the equation

$$k_{ii} = CS^{x} \qquad (3.2)$$

except for k_{22} and k_{33} of 8CB which diverge as T_{AN} is approached. However the k_{33} values of 7CB and k_{11} of 8CB do not fit *vary* well *to* this equation. Hence in those *two* cases the curves In the figures are not the fitted ones. The temperature variation of k_{11}, k_{22} and k_{33} are plotted in figures 3.8, 3.9 and 3.10 respectively. The curves *except* in those cases mentioned above indicate the variations according to equation (3.2).

Before we discuss *our* results, it is worthwhile summarizing some of the significant results from recent X-ray diffraction measurements (Leadbetter et al. 1975) on 5CB and 7CB in nematic as well as isotropic phases.

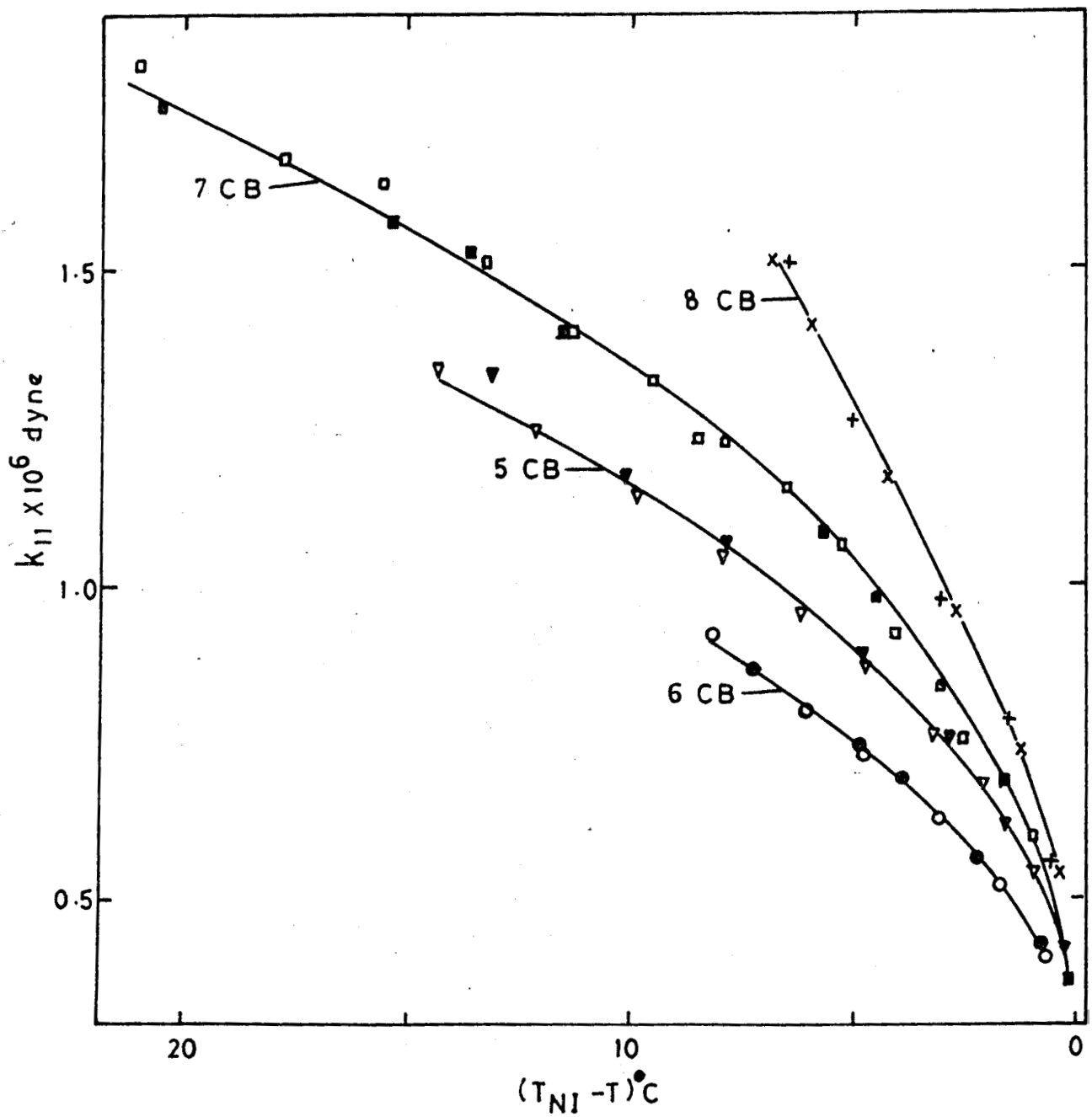

Figure 3.8

Variation of the splay elastic constant, k_{11} as a function of the relative temperature for 5CB-8CB.

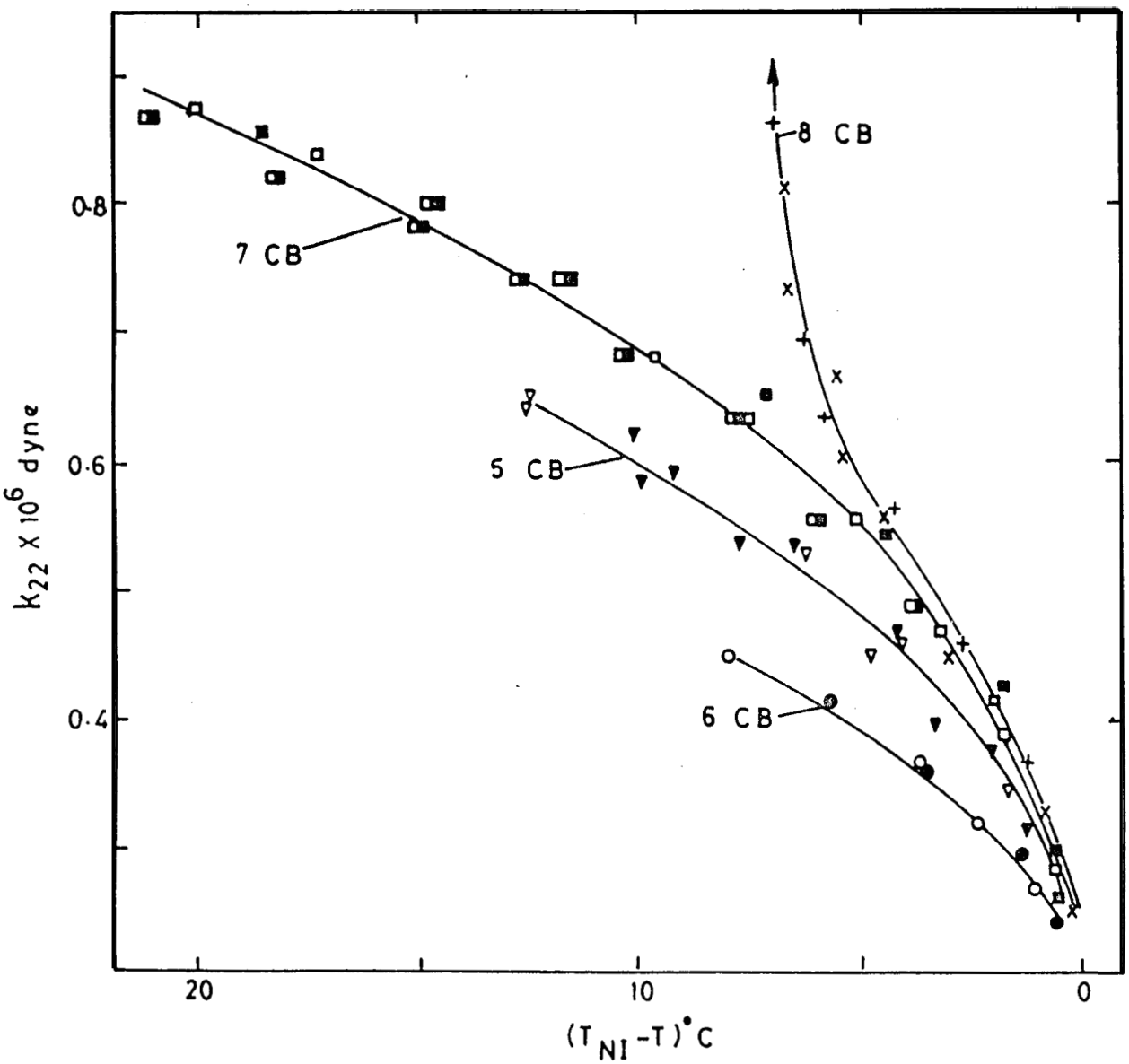

Figure 3.9

Variation of the twist elastic constant k_{22} as a function of the relative temperature for 5CB-8CB.

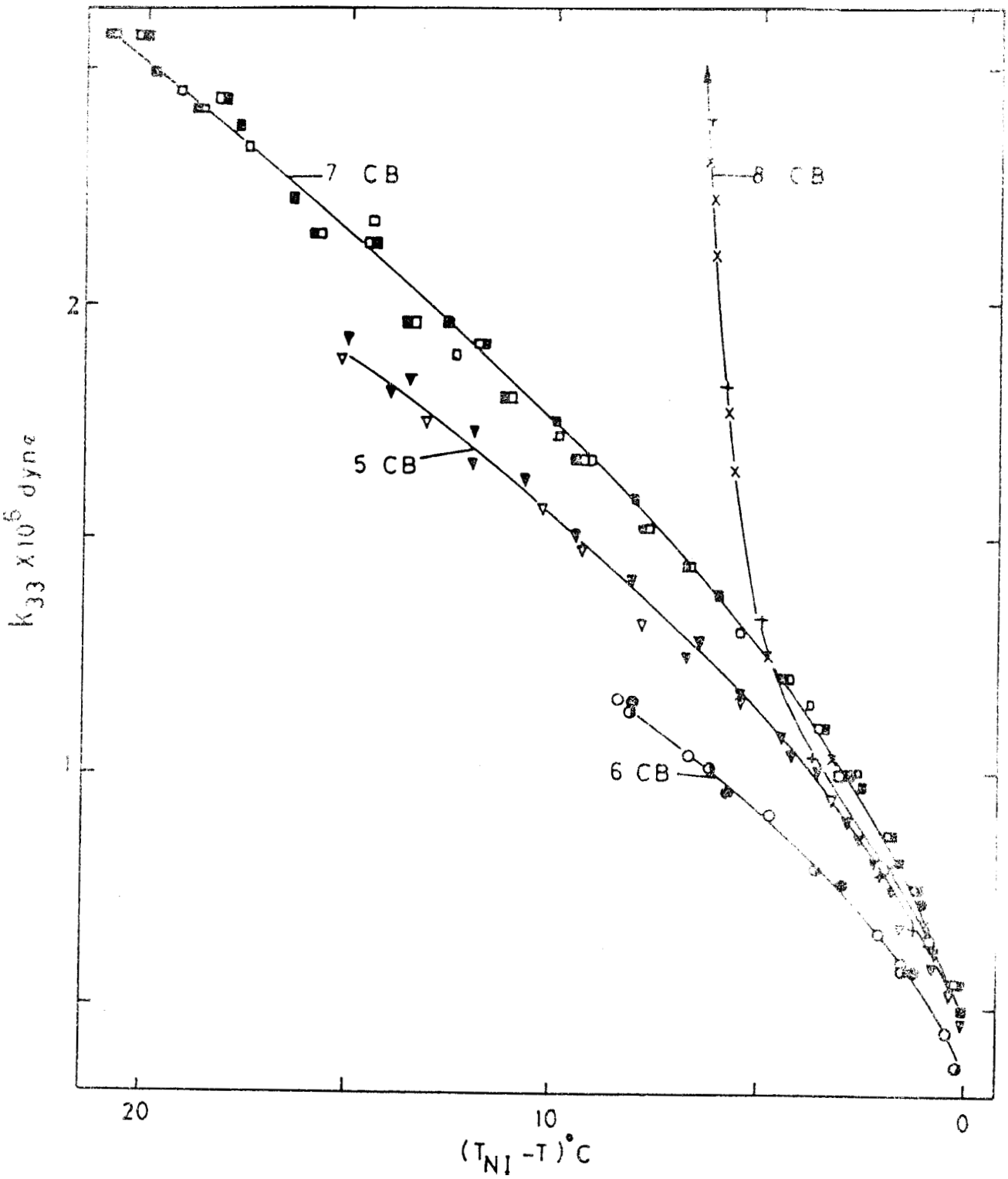

Figure 3.10

Variation of the **bend** elastic constant k_{33} **as a** function **of the** relative temperature for 5CB-8CB.

It was found that the integrated intensity of equatorial (1E) reflections and their width in the equatorial plane change little with temperature, even when the sample was taken *to* the isotropic phase. This implies that the lateral ordering of the molecules remains unchanged. From the width of 1E reflections it wale estimated that the lateral correlation length (L_r) is $\sim$ 9 times the mean near neighbour distance in this direction.

Both 7CB and 5CB show strong but diffuse meridional (1M) reflections which are temperature sensitive. As the temperature Is decreased, the peak intensity increases while its width decreases. This shows that the longitudinal order increases with the decrease in temperature which also means that the molecular end chains become stiffer. 1M reflection of 5CB is slightly weaker than that of 7CB. The peak widths indicate that the longitudinal correlation lengths (L_d) is $\sim$ 4-5 times the Bragg spacing. Another important result is that the Bragg spacing *is* about 1.4 times the molecular length. This suggests strong antiparallel ordering of the molecules (figure 3.11) confirming an idea that was first put forward By Madhusudana and Chandrasekhar (1973). X-ray diffraction data on 8CB in smectic phase (Crag and Lydon 1974) also

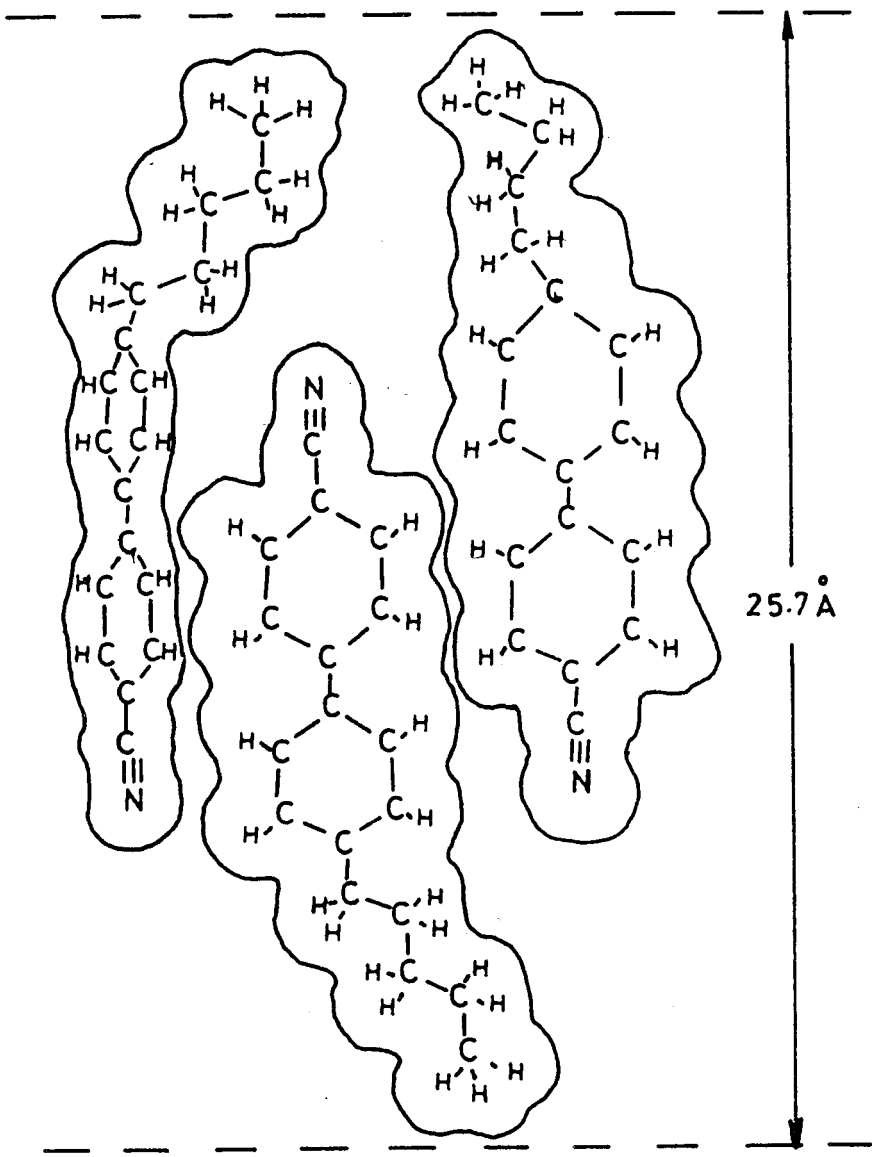

Figure 3.11

Schematic diagram of suggested local structure in 5CB (and 7CB) resulting in a repeat distance along the texture axis of ~ 1.4 molecular lengths with highly mobile alkyl chains and a tendency to local layer formation. (Reproduced from Leadbetter et al. J. de Phys. 01-37, 1975.)

gives a layer thickness ~1.4 times the molecular length. So far no one appears to have obtained the X-ray data on 6CB and 8CB in the nematic and isotropic phases.

We shall now consider our results. For the sake of comparison, we have plotted the values of T_{NI} and the corresponding latent heats in figure 3.12. In the lower part of the figure the elastic constants and the order parameters at $T_{NI}-T = 2°C$ are plotted as functions of the number of carbon atoms in the end chain. From the figure we make the following observations.

The transition temperatures show the usual odd even effect. Among the elastic constants only k_{33} shows this trend. The order parameter alternates for the first three members but increases on going from 7CB to 8CB. ΔH, k_{11} and k_{22} have the same trend as S. We shall discuss these trends in detail at a later stage.

The values of C and x (eqn.(3.2)) for different compounds and elastic constants are given in Table 3.11. In all the cases both C and x show the odd-even effect. The index x is greatest for k_{33} and least for k_{22}.

We have calculated the ratios of elastic constants for various relative temperatures. They are

tabulated in table 3.12. If the mean field theory is obeyed, the ratios should be independent of temperature. The table shows that this is not the case.

We will now discuss our results keeping in mind ths X-ray diffraction data. We will first consider only 5CB, 6OB and 7CB.

(a) Table 3.11 shows that bend constant does not follow the mean field result ($k_{ii} \propto S^2$) in any of the compounds. The index x is always greater than 2. This can be understood in terms of the longitudinal correlation in the cybotactic group becoming stronger at lower temperatures as evidenced by the sharper and narrower meridional reflectiones. From the nature of bend deformations (figure 1.2) one can see that if effective length of the molecule increases, the bend constant also increases. (In fact the hard *rod* model would lead *to* this result (Onsager 1932, Zwanzig 1963). Gruler (1975) has also arrived at a similar result using an argument based on mean field theory.) Thus one can expect that the bend constant takes higher values at lower temperatures than those indicated by the mean field theory. Further, the odd-even effect in both C and x, might mean that the cybotactic groups are stronger in the odd members.

However we have no X-ray data available for 6CB to check this point. The increase in both C and x between 5CB and 7CB can be understood in terms of the larger cybotactic groups in tho latter ($\sim$ 150 molecules) compared to the former ($\sim$ 100 molecules).

(b) The splay constant exhibits a behaviour close to the mean field trend. The deviation of x from 2 can again be understood in terms of the nature of the deformation (figure 1.2). The elastic constant should slightly increase with the effective length of the molecules.

(c) The twist constant has the mean field type of variation in 5CB and 7CB. However x is lower than 2 in the case of 6CB and moreover C is much smaller than those in 5CB and 7CB. Apart from pointing out that the cybotactic order in this compound is likely to be much less than in other cases, we do not offer any explanation for this lowering of x in 6CB.

We will now compare the ratios of the elastic constants in these three compounds (Table 3.12). In spite of the considerably different values of C and x, corresponding to different elastic constants in a given compound as well as the same elastic constant of different compounds, it is remarkable that the ratios of elastic constants turn out to be practically the

same for all the cases at the same relative temperature (T_{NI} - . It means that even though the actual 'strength' of the cybotactic order is different in the three compounds, the groups grow in a rather similar fashion in all the three cases as the temperature is lowered. The rapid increase in k_{33}/k_{22} and a somewhat slower increase of k_{33}/k_{11} as well as thr slow increase of k_{11}/k_{22} can be understood in terms of the strengthening of the cybotactic order in the longitudinal direction as the temperature is lowered and the nature of the *three* deformatione (figure 1.2).

We shall now discuss the elastic constants of 8CB near T_{NI} (figure 3.12). (The behaviour near T_{AN} will be dealt with in detail In Chapter V.) We hare already pointed out that k_{33} and T_{NI} for this compound are lower than those of 7CB, i.e., the odd-even effect extends to 8CB for these properties. As pointed out earlier, k_{33} may be particularly sensitive to the disposition *of* the end group in view of the nature of the deformation induced. The increase in S, k_{11} and k_{22} from 7CB to 8CB can be understood if we assume that the lateral correlation length of the cybotactic group increases in 8CB compared to that in 7CB close to T_{NI}. It is interesting to note that

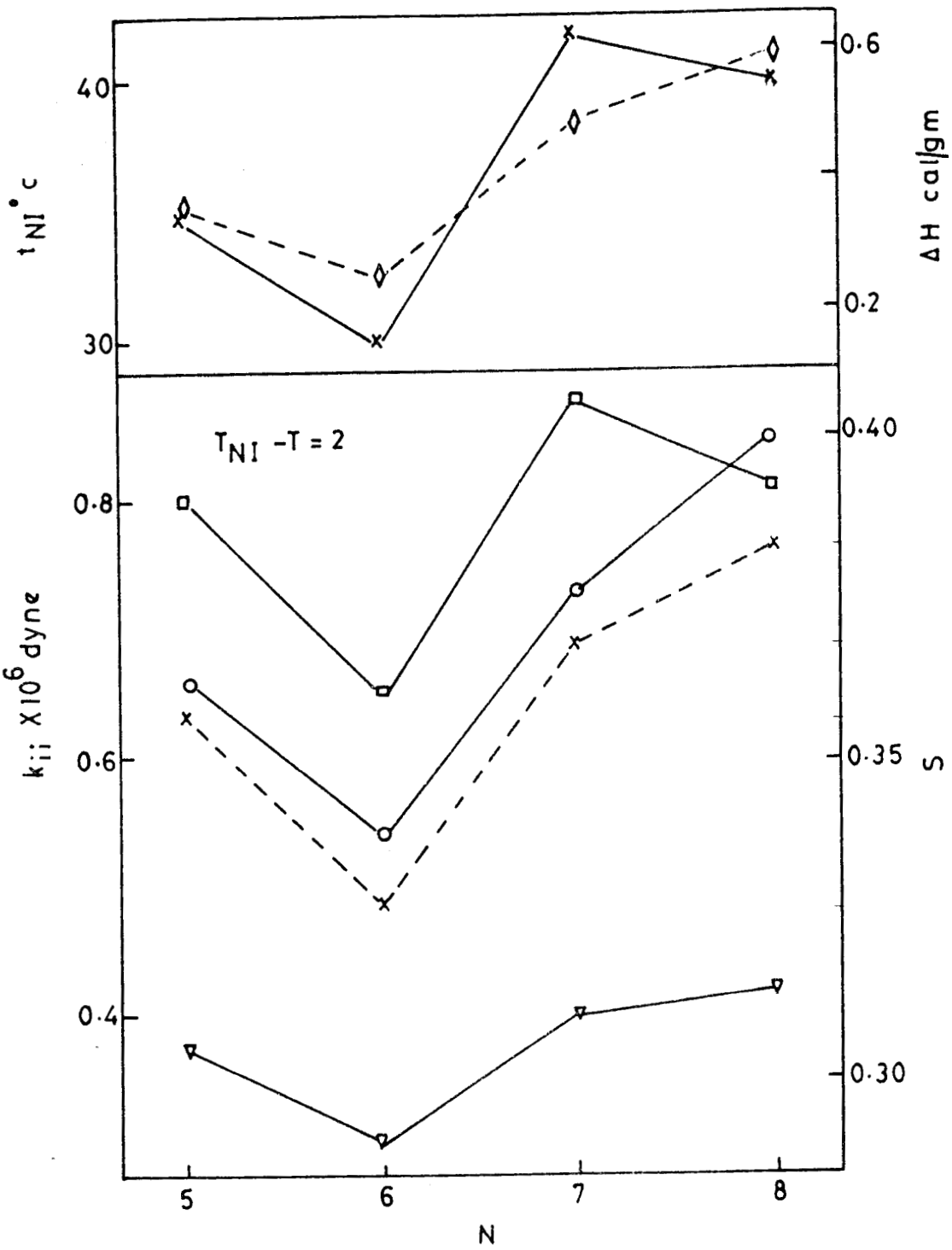

Figure 3.12

The nematic-isotropic transition points ($^{\times}$), the heats of transition ($\diamond$), the order parameters ($\times$), splay elastic constants (o), twist elastic constants (∇) and the bend elastic constants ($\square$) of 5CB-8CB as functions of the number of carbon atoms in the end chain. The parameters in the lower section of the diagram are those at $T_{NI} - T = 2°C$.

the decrease in k_{33} and increase in k_{11} in 8 CB compared to the previous member is such that $k_{11} > k_{33}$ close to T_{NI}. (This can also be seen from table 3.92 where the ratios of elastic constants are shown.) This result appears to Be quite unusual. As the temperature is decreased, however, cybotactic like order grows in size with a rapid increase in both the transverse and longitudinal correlation lengths ($\xi_{\perp}$ and $\xi_{\parallel}$) which will lead to the divergence of k_{22} and k_{33} close to T_{AN}. However as lo to be expected in such cases, k_{11} behaves in the normal manner so that k_{33} becomes greater than k_{11} at $T_{NI} - T = 4.5°C$.

References

Barrall, E.M., Johnson, J.F. 1974 'Liquid Crystals and Plastic Crystals', Vol. 2, Ch.10, eds. G.W.Gray and P.A.Winsor (John Wiley & Sons).

Chandrasekhar, S. and Madhusudana, N.V. 1969 J. de Physique 30, C4-24.

Cheung, L., Meyer, R.E. 1973 Phys.Lett. 43A, 261.

de Vries, A 1973 Proc. International Liquid Crystals Conference, Bangalore - Pramana Supplement 1, 93 1975.

Gray, G.W., Harrison, K.J. and Nash, J.A. 1973 Electron Lett. 9, 130.

Gray, G.W., Harrison, K.J., Nash, J.A., Constant, J., Hulme, D.S., Kirton, J. and Raynes, E.P. 1974 Proc. Symp. Ordered Fluids and Liquid Crystals, 1973, eds. R.S. Porter and J.F.Johnson, p. 617.

Grey, G.W. and Lydon, J.E. 1974 Nature 252, 221.

Gruler, H. 1973 Z. Naturforsch. 28a, 474.

Gruler, H. 1975 Z. Naturforsch. 30a, 230.

Guyon, E., Pieranski, P. and Boix, M. 1973 Lett. Appl. Engg. Sci. 1, 19.

Heger, J.P. 1975 J. de Physique Lett. 36, L-209.

Janning, J.L. 1972 Appl. Phys. Lett. 4, 173.

Lonsdale, K. 1937 Reports on Progress in Phys. IV, 368.

Leadbetter, A.J., Richardson, R.M. and Colling, C.N. 1975 J. de Physique C1-37

Lippman, H, and Weber, K.H. 1957 Ann. Phys. Lpz. 20, 265.

Madhusudana, N.V., Shashidhar, R. and Chandrasekhar, S. 1971 Mol. Cryst. Liq. Cryst. 13, 61.

Madhusudana, N.V. and Chandrasekhar, S. 1975 Proc. International Liquid Crystals Conference, Bangalore, 1973 - Pramana Supplement 1, 57.

Marcelja, S. 1974 J. Chem. Phys. 60, 3599.

Onsager, L. 1932 Phys. Rev. 38, 2265.

Pallet, O. and Chatelain, P. 1970 Bull. Soc. Fr. Miner. Cryst. 73, 154.

Pines, A., Ruben, D.J. and Allison, S. 1975 Rep. U.S. Atomic Energy Commission, Contract W7405-ENG48.

Zwanzig, R. 1963 J. Chem. Phys. 39, 1714.

Table 3.1

Transition temperatures *and* latent heats of transition of 4'-n-alkyl-4-cyanobiphenyls (nCB)

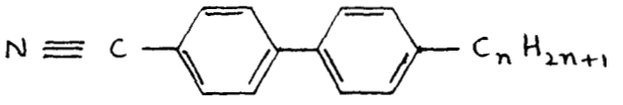

	Transition temperatures (°C)			Latent heats *of* transition ΔH_{NI} cal/*gm*
	Crystal-nematic or crystal-smectic	smectic-nematic	nematic-isotropic	
5CB	22.4	-	34.5	0.33
6CB	13.8	-	28.8	0.24
7CB	28.5	-	41.9	0.48
8CB	20.5	33.3	40.1	0.59

Table 3.2

Anisotropy *of* diamagnetic susceptibility in *n*CB

	5CB	6CB	7CB	8CB
$\Delta\chi_{om} \times 10^7$ c.g.s.units	4.76	4.50	4.28	4.07

Table 3.3: Refractive indices of nCB

(i) 5CB

$(T_{NI}-T)$ in °C	λ 5461 Å		λ 5893 Å		λ 6328 Å	
	n_o	n_e	n_o	n_e	n_o	n_e
14.6 (II)*	1.536	1.739	1.532	1.727	1.528	1.719
14.4 (I)	1.536	1.737	1.532	1.726	1.528	1.717
13.1 (I)	1.537	1.734	1.532	1.723	1.528	1.714
12.2 (II)	1.538	1.733	1.533	1.722	1.528	1.713
10.7 (I)	1.539	1.727	1.533	1.716	1.530	1.708
10.3 (II)	1.539	1.727	1.534	1.716	1.530	1.708
8.2 (II)	1.540	1.721	1.535	1.711	1.531	1.702
7.6 (I)	1.541	1.718	1.536	1.707	1.531	1.698
6.0 (II)	1.542	1.714	1.536	1.703	1.532	1.695
5.4 (I)	1.542	1.712	1.537	1.701	1.533	1.693
3.5 (II)	1.544	1.703	1.539	1.693	1.535	1.685
2.8 (I)	1.546	1.699	1.541	1.685	1.537	1.680
1.4 (II)	1.550	1.689	1.544	1.679	1.540	1.672
0.1 (II)	1.557	1.670	1.551	1.662	1.547	1.656

*I and II in parentheses refer to two independent measurements.

(ii) 6CB

$(T_{NI}-T)$ in °C	λ 5461 Å		λ 5893 Å		λ 6328 Å	
	n_o	n_e	n_o	n_e	n_o	n_e
8.4 (I)	1.540	1.703	1.535	1.692	1.531	1.684
8.1 (II)	1.540	1.703	1.535	1.692	1.531	1.684
6.3 (I)	1.542	1.695	1.537	1.686	1.533	1.679
5.4 (II)	1.543	1.693	1.538	1.683	1.534	1.675
3.9 (I)	1.545	1.687	1.540	1.677	1.536	1.669
3.4 (II)	1.546	1.683	1.541	1.673	1.537	1.666
2.5 (I)	1.547	1.679	1.542	1.670	1.538	1.663
1.9 (II)	1.548	1.675	1.543	1.667	1.539	1.659
1.3 (I)	1.550	1.671	1.545	1.662	1.541	1.654
0.4 (II)	1.555	1.659	1.550	1.651	1.545	1.645

Table 3.3 contd..

(iii) 7CB

$(T_{NI}-T)$ in °C		λ 5461 Å		λ 5893 Å		λ 6328 Å	
		n_o	n_e	n_o	n_e	n_o	n_e
20.0	(II)	1.523	1.719	1.519	1.709	1.516	1.701
19.4	(I)	1.524	1.718	1.519	1.707	1.516	1.699
18.2	(I)	1.524	1.716	1.519	1.705	1.516	1.697
17.4	(II)	1.524	1.714	1.520	1.704	1.516	1.696
15.1	(I)	1.524	1.710	1.520	1.700	1.517	1.692
14.3	(II)	1.525	1.708	1.520	1.698	1.517	1.690
12.4	(I)	1.525	1.705	1.520	1.695	1.517	1.687
11.3	(II)	1.525	1.702	1.521	1.692	1.518	1.685
10.0	(I)	1.526	1.699	1.521	1.689	1.518	1.682
8.5	(II)	1.527	1.696	1.522	1.686	1.519	1.679
7.2	(I)	1.527	1.692	1.523	1.682	1.519	1.675
6.2	(II)	1.528	1.689	1.524	1.680	1.520	1.672
4.9	(I)	1.529	1.685	1.525	1.675	1.521	1.668
4.5	(II)	1.530	1.682	1.526	1.673	1.522	1.665
3.3	(I)	1.532	1.677	1.527	1.667	1.524	1.660
2.9	(II)	1.533	1.673	1.528	1.664	1.525	1.657
2.0	(I)	1.535	1.669	1.530	1.660	1.526	1.653
1.2	(II)	1.539	1.658	1.533	1.651	1.529	1.645

(iv) 8CB

6.3	(II)	1.525	1.682	1.520	1.673	1.517	1.666
5.1	(I)	1.526	1.676	1.521	1.667	1.518	1.659
4.2	(II)	1.527	1.672	1.523	1.663	1.520	1.657
3.0	(II)	1.529	1.667	1.525	1.658	1.521	1.651
2.7	(I)	1.530	1.666	1.524	1.657	1.521	1.651
1.5	(I)	1.532	1.659	1.527	1.651	1.523	1.643
1.2	(II)	1.535	1.653	1.530	1.645	1.526	1.639
0.2	(I)	1.537	1.643	1.533	1.636	1.529	1.630
-0.2	(I)	1.572		1.566		1.560	

Table 3.4

Densities and average polarizabilities of nCB

	ρ at 25°C in gm/cc	$\bar{\alpha} \times 10^{24}$ cm^3		
		λ 5461 Å	λ 5893 Å	λ 6328 Å
5CB	1.023*	33.2	32.86	32.63
6CB	1,012	34.98	34.63	34.38
7CB	1.010*	36.75	36.40	36.13
8CB	0.995 (at 35°C)	38.53	38.17	37.88

*measured values

Table 3.5: Density of nCB (gm/c.c.)

(i) 5CB

$T_{NI}-T$ °C	λ 5461 Å	λ 5893 Å	λ 6328 Å	Mean
14.4	1.0266	1.0276	1.0272	1.0271
13.1	1.0260	1.0264	1.0263	1.0262
10.7	1.0239	1.0246	1.0239	1.0241
7.6	1.0209	1.0219	1.0209	1.0212
5.5	1.0197	1.0203	1.0197	1.0199
2.8	1.0167	1.0173	1.0169	1.0170
14.6	1.0278	1.0285	1.0281	1.0281
12.2	1.0257	1.0264	1.0254	1.0258
10.3	1.0239	1.0246	1.0242	1.0242
8.3	1.0218	1.0228	1.0221	1.0222
6.1	1.0200	1.0207	1.0200	1.0202
3.6	1.0173	1.0182	1.0178	1.0178
1.4	1.0150	1.0158	1.0151	1.0153
0.1	1.0126	1.0134	1.0136	1.0132

(ii) 6CB

8.5	1.0157	1.0166	1.0164	1.0162
6.3	1.0139	1.0145	1.0149	1.0144
4.0	1.0118	1.0127	1.0128	1.0124
2.5	1.0103	1.0112	1.0116	1.0110
1.4	1.0091	1.0103	1.0098	1.0098
8.1	1.0157	1.0166	1.0167	1.0163
5.4	1.0133	1.0142	1.0143	1.0139
3.4	1.0112	1.0118	1.0125	1.0118
1.9	1.0097	1.0109	1.0110	1.0105
0.4	1.0080	1.0091	1.0091	1.0087

Table 3.5 contd..

(iii) 7CB

$T_{NI}-T$ °C	λ 5461 Å	λ 5893 Å	λ 6328 Å	Mean
19.4	1.0111	1.0115	1.0120	1.0115
18.3	1.0102	1.0105	1.0108	1.0105
15.1	1.0078	1.0081	1.0090	1.0083
12.4	1.0057	1.0063	1.0065	1.0062
10.0	1.0036	1.0042	1.0050	1.0043
7.2	1.0015	1.0024	1.0029	1.0023
4.9	0.9994	1.0003	1.0011	1.0003
3.3	0.9982	0.9985	0.9992	0.9986
2.0	0.9970	0.9976	0.9977	0.9974
20.0	1.0117	1.0127	1.0129	1.0024
17.4	1.0097	1.0102	1.0105	1.0101
14.3	1.0072	1.0078	1.0084	1.0078
11.3	1.0048	1.0054	1.0062	1.0054
8.5	1.0030	1.0039	1.0041	1.0037
6.2	1.0012	1.0020	1.0023	1.0018
4.5	0.9994	1.0006	1.0001	1.0000
2.9	0.9973	0.9982	0.9986	0.9980
1.2	0.9955	0.9960	0.9965	0.9960

(iv) 8CB

5.1	0.9943	0.9949	0.9958	0.9950
2.7	0.9925	0.9927	0.9939	0.9930
1.6	0.9913	0.9921	0.9921	0.9918
0.2	0.9892	0.9900	0.9915	0.9902
-0.2	0.9856	0.9876	-	0.9866
6.3	0.9967	0.9970	0.9979	0.9972
4.2	0.9940	0.9946	0.9958	0.9948
3.0	0.9928	0.9937	0.9942	0.9936
1.2	0.9910	0.9918	0.9927	0.9918

Table 3.6

$\Delta\alpha$ and $(\bar{\alpha}/\Delta\alpha)$ for the different members of nCB

	5CB	6CB	7CB	8CB
$\Delta\alpha \times 10^{24}$ cm^3	26.98	26.90	27.16	27.08
$\frac{\bar{\alpha}_{5893}}{\Delta\alpha}$	1.22	1.29	1.34	1.41

Table 3.7

Order parameter of nCB

I(1) 5CB	Order parameter S			
$T_{NI}-T$ °C	λ5461 Å	λ5893 Å	λ6328 Å	Mean
14 4	0.496	0.496	0.496	0.496
13 1	0.486	0.487	0.488	0.487
10 7	0.467	0.468	0.468	0.468
7.6	0.440	0.440	0.440	0.440
5.5	0.421	0.420	0.422	0.421
2.8	0.380	0.380	0.378	0.379
14.6	0.499	0.499	0.499	0.499
12.2	0.484	0.484	0.484	0.484
10.3	0.466	0.468	0.468	0.467
8.3	0.450	0.452	0.452	0.451
6.1	0.429	0.428	0.429	0.429
3.6	0.396	0.394	0.395	0.395
1.4	0.347	0.348	0.349	0.348
0.1	0.282	0.284	0.288	0.285
(Δi) 6CB				
8 5	0.429	0.428	0.427	0.428
6 3	0.405	0.407	0.408	0.407
4.0	0.376	0.375	0.373	0.375
2.5	0.350	0.350	0.350	0.350
1.4	0.321	0.320	0.318	0.320
8.1	0.429	0.430	0.431	0.430
5.4	0.397	0.396	0.394	0.396
3.4	0.362	0.363	0.362	0.362
1.9	0.337	0.337	0.336	0.337
0.4	0.274	0.277	0.279	0.277

Table 3.7 contd..

$T_{NI}-T$ °C	λ5461 Å	λ5893 Å	λ6328 Å	Mean
(iii) 7CB				
19.4	0.540	0.540	0.540	0.540
18.2	0.533	0.534	0.533	0.533
15.2	0.519	0.517	0.517	0.518
12.4	0.502	0.501	0.502	0.501
10.0	0.483	0.483	0.484	0.483
7.2	0.460	0.459	0.461	0.460
4.9	0.435	0.434	0.434	0.434
3.3	0.405	0.405	0.406	0.405
2.0	0.377	0.376	0.377	0.377
20.0	0.543	0.542	0.542	0.543
17.4	0.528	0.528	0.530	0.529
14.3	0.511	0.510	0.511	0.511
11.3	0.493	0.492	0.494	0.493
8.5	0.471	0.471	0.473	0.472
6.2	0.449	0.448	0.448	0.448
4.5	0.425	0.424	0.424	0.424
2.9	0.391	0.392	0.393	0.392
1.2	0.335	0.341	0.346	0.341
(iv) 8CB				
5.1	0.445	0.445	0.444	0.445
2.7	0.405	0.406	0.408	0.406
1.6	0.380	0.378	0.380	0.379
0.2	0.310	0.314	0.318	0.314
6.3	0.467	0.467	0.468	0.468
4.2	0.430	0.429	0.432	0.430
3.0	0.409	0.408	0.410	0.409
1.2	0.349	0.354	0.358	0.354

Table 3.8: Splay elastic constant of nCB

$T_{NI}-T$ °C	H_c Kgauss	$k_{11} \times 10^6$ dyne	$(k_{11})_{cal} \times 10^6$ dyne
(i) 5CB			
14.3	2.61	1.33	1.32
12.1	2.56	1.24	1.24
9.8	2.48	1.12	1.15
7.9	2.43	1.04	1.06
6.1	2.38	0.95	0.97
4.7	2.33	0.87	0.89
3.1	2.25	0.76	0.77
2.0	2.20	0.68	0.66
0.9	2.05	0.53	0.53
x_o = 28.2 µm			
13.1	2.63	1.32	1.28
10.1	2.53	1.16	1.16
7.8	2.46	1.05	1.05
4.7	2.35	0.88	0.89
2.7	2.27	0.75	0.73
1.5	2.15	0.61	0.60
0.1	1.96	0.42	0.40
x_o = 28.1 µm			
(ii) 6CB			
8.1	2.56	0.92	0.91
6.0	2.46	0.80	0.81
4.7	2.40	0.73	0.74
3.1	2.30	0.62	0.63
1.7	2.20	0.52	0.53
0.6	2.07	0.42	0.41
x_o = 26.7 µm			
7.3	2.51	0.86	0.87
4.8	2.43	0.75	0.74
3.8	2.38	0.69	0.68
2.2	2.25	0.56	0.57
0.7	2.1	0.43	0.42
x_o = 26.6 µm			

Table 3.8 continued..

$T_{NI}-T$ °C	H_o Kgauss	$k_{11} \times 10^6$ dyne	$(k_{11})_{cal} \times 10^6$ dyne
(iii) 7CB			
21.1	3.03	1.82	1.80
17.9	2.95	1.67	1.67
15.6	2.95	1.63	1.59
13.3	2.88	1.51	1.50
11.0	2.82	1.40	1.40
9.5	2.77	1.32	1.32
7.8	2.70	1.22	1.23
6.5	2.66	1.15	1.15
5.2	2.61	1.06	1.06
4.0	2.48	0.92	0.95
2.6	2.40	0.75	0.82
1.0	2.22	0.59	0.56
x_o = 28.7			
20.6	3.03	1.75	1.77
15.4	2.95	1.57	1.58
13.6	2.93	1.52	1.51
11.5	2.85	1.40	1.41
8.5	2.75	1.23	1.27
5.7	2.66	1.08	1.10
4.5	2.59	0.98	0.99
3.0	2.48	0.84	0.85
1.6	2.36	0.69	0.67
0.2	2.12	0.37	0.27
x_o = 28.2 μm			
(iv) 8 CB			
6.8	3.27	1.52	
5.9	3.17	1.40	
4.2	3.00	1.17	
2.6	2.82	0.96	
1.1	2.61	0.74	
0.4	2.35	0.54	
x_o = 27.1			
6.5	3.27	1.50	
5.0	3.05	1.26	
3.0	2.82	0.97	
1.5	2.66	0.79	
0.5	2.37	0.56	
x_o = 27.1			

Table 3.9: Twist elastic constant of nOB

(i) 5OB

$T_{NI}-T$ °C	H_c Kgauss	$k_{22} \times 10^6$ dyne	$(k_{22})_{cal} \times 10^6$ dyne
12.3	2.27	0.65	0.64
9.0	2.22	0.59	0.58
6.1	2.17	0.52	0.51
4.0	2.07	0.45	0.45
1.6	1.94	0.34	0.34
0.4	1.81	0.26	0.25
x_o = 23 µm			
12.4	2.2	0.64	0.65
9.8	2.15	0.58	0.60
7.6	2.1	0.53	0.55
4.7	1.99	0.44	0.47
3.1	1.94	0.39	0.41
1.2	1.87	0.31	0.31
x_o = 23.5 µm			
9.9	2.27	0.62	0.60
6.4	2.17	0.53	0.52
4.1	2.10	0.46	0.45
1.9	2.00	0.37	0.36
0.5	1.87	0.27	0.26
x_o = 23 µm			

(ii) 6OB

5.5	2.07	0.41	0.40
3.3	1.99	0.35	0.34
1.2	1.87	0.27	0.27
0.5	1.81	0.23	0.23
x_o = 22.8 µm			
7.8	2.12	0.44	0.45
3.5	2.02	0.36	0.35
2.2	1.94	0.31	0.31
0.9	1.87	0.26	0.26
x_o = 22.5 µm			

Table 3.9 continued

$T_{NI}-T$ °C	Kgauss	$k_{22} \times 10^6$ dyne	$(k_{22})_{cal} \times 10^6$ dyne
		(111) 7CB	
19.8	2.4	0.88	0.87
17.1	2.38	0.84	0.83
14.7	2.35	0.80	0.78
11.8	2.30	0.74	0.73
9.5	2.25	0.68	0.69
7.4	2.20	0.63	0.63
5.1	2.12	0.55	0.56
3.1	2.02	0.46	0.48
1.7	1.94	0.38	0.38
0.6	1.81	0.28	0.28
x_o = 25.4 µm			
21.0	2.4	0.87	0.89
18.0	2.37	0.82	0.84
14.8	2.35	0.78	0.78
12.5	2.32	0.74	0.74
10.1	2.27	0.68	0.70
7.7	2.22	0.68	0.70
5.9	2.12	0.55	0.59
3.7	2.07	0.48	0.50
1.8	2.02	0.41	0.39
0.4	1.81	0.26	0.25
x_o = 25.1 µm			
18.4	2.46	0.86	0.85
14.4	2.43	0.80	0.78
11.3	2.38	0.74	0.72
7.1	2.33	0.65	0.62
4.4	2.20	0.54	0.53
2.0	2.07	0.42	0.41
0.6	1.89	0.29	0.27
x_o = 24.6 µm			

Table 3.9 continued

$T_{NI}-T$ °C	H_c Kgauss	$k_{22} \times 10^6$ dyne
	(iv) 8CB	
6.83	3.07	1.13
6.70	2.61	0.81
6.52	2.48	0.73
5.76	2.38	0.66
5.28	2.30	0.60
4.34	2.23	0.55
2.93	2.07	0.44
0.71	1.92	0.32
0.12	1.80	0.24
x_o = 24.9 µm		
6.73	2.72	0.86
6.08	2.46	0.69
5.65	2.38	0.63
4.10	2.30	0.56
2.52	2.15	0.45
1.10	2.02	0.36
0.39	1.87	0.28
x_o = 24.5 µm		

Table 3.10: Bend elastic constant of nCB

(1) 5CB

$T_{NI}-T$ °C	H_c Kgauss	$k_{33}\times10^6$ dyne	$(k_{33})_{cal}\times10^6$ dyne
15.3	3.17	1.88	1.91
13.1	3.10	1.74	1.75
10.3	3.0	1.56	1.57
7.9	2.82	1.31	1.39
5.5	2.72	1.15	1.19
3.2	2.56	0.94	0.95
1.8	2.38	0.74	0.75
0.4	2.20	0.53	0.48
x_o = 27.4 μm			
15.0	3.22	1.93	1.89
12.0	3.10	1.72	1.67
9.5	2.97	1.50	1.50
6.6	2.82	1.28	1.28
4.5	2.68	1.07	1.10
2.7	2.50	0.87	0.89
0.7	2.30	0.60	0.54
0.1	2.10	0.46	0.42
x_o = 27.4 μm			
14.0	3.45	1.81	1.81
12.0	3.36	1.66	1.67
9.3	3.24	1.47	1.49
6.8	3.07	1.25	1.29
5.1	2.94	1.09	1.15
3.6	2.87	1.00	0.99
2.1	2.70	0.80	0.80
0.7	2.43	0.57	0.54
x_o = 24.9 μm			
13.6	3.5	1.84	1.78
10.8	3.34	1.61	1.60
8.1	3.20	1.41	1.40
5.5	3.02	1.17	1.19
4.2	2.92	1.04	1.06
2.6	2.75	0.86	0.87
1.4	2.60	0.67	0.68
0.1	2.30	0.46	0.42
x_o = 24.9 μm			

Table 3.10 continued

(ii) 6CB

$T_{NI}-T$ °C	H_c Kgauss	$k_{33} \times 10^6$ dyne	$(k_{33})_{cal} \times 10^6$ d ~ —
8.5	3.0	1.15	1.16
6.7	2.94	1.04	1.04
4.6	2.82	0.91	0.89
2.1	2.56	0.65	0.67
1.5	2.50	0.59	0.60
0.4	2.32	0.44	0.43
x_o = 25.2 μm			
8.0	3.04	1.16	1.14
5.8	2.87	0.96	0.97
2.9	2.70	0.76	0.74
1.1	2.48	0.57	0.55
0.4	2.33	0.44	0.43
x_o = 25.2 μm			
8.0	3.01	1.14	1.14
6.2	2.92	1.01	0.99
3.6	2.70	0.79	0.81
1.4	2.45	0.57	0.59
0.1	2.17	0.37	0.37
x_o = 25.2 μm			

(iii) 7CB

19.2	4.1	2.45
17.5	4.03	2.33
15.3	3.94	2.18
12.5	3.75	1.90
10.0	3.64	1.73
7.7	3.48	1.51
5.5	3.31	1.30
3.2	3.04	1.0
2.2	3.00	0.84
0.9	2.80	0.68
x_o = 24.9 μm		

(iii) 7CB continued ....

Table 3.10 continued

(iii) 7CB

$T_{NI}-T$ °C	H_c Kgauss	$k_{33} \times 10^6$ dyne
19.8	4.12	2.49
17.8	4.05	2.37
16.4	3.96	2.22
12.8	3.80	1.96
10.1	3.66	1.75
8.1	3.55	1.59
6.0	3.38	1.37
3.9	3.22	1.16
2.6	3.07	0.98
1.6	2.92	0.81
1.1	2.82	0.72
0.3	2.6	0.52
x_o = 24.9 μm		
20.8	4.23	2.58
18.7	4.12	2.41
15.8	3.96	2.15
13.5	3.82	1.95
11.1	3.73	1.80
9.4	3.64	1.67
6.8	3.47	1.44
4.3	3.30	1.21
2.8	3.12	1.00
1.1	2.90	0.75
x_o = 24.5 μm		
20.0	4.23	2.57
18.1	4.16	2.44
14.6	3.96	2.12
11.9	3.82	1.91
9.2	3.66	1.68
6.0	3.43	1.38
3.4	3.19	1.09
1.8	2.99	0.86
0.4	2.66	0.53
x_o = 24.5 μm		

Table 3.10 continued

(iv) 8CB

$T_{NI}-T$ °C	H_o Kgauss	$k_{33}x10^6$ dyne
6.75	3.57	6.17
6.57	2.75	3.63
6.47	2.53	3.07
6.25	2.2	2.30
6.17	2.17	2.23
5.74	1.94	1.76
5.54	1.88	1.64
4.69	1.66	1.24
3.08	1.56	1.02
1.82	1.43	0.79
0.96	1.35	0.66
0.34	1.28	0.54
x_o = 50 µm		
6.65	2.87	3.98
6.47	2.53	3.07
6.32	2.24	2.39
6.12	2.10	2.09
5.84	1.97	1.82
5.64	1.94	1.75
4.94	1.71	1.33
3.67	1.54	1.03
2.06	1.41	0.79
1.20	1.35	0.67
0.22	1.25	0.49
x_o = 50 µm		

Table 3.11: The experimental values fitted to the equation $k_{ii} = CS^x$

	k_{11}		k_{22}		k_{33}	
	C	x	C	x	C	x
5CB	5.98	2.15	2.70	1.96	11.78	2.65
6CB	5.31	2.08	2.00	1.74	8.40	2.35
7CB	7.18	2.31	3.00	2.01	13.81	2.81
8CB	10.79	2.62				

Table 3.12: Ratios of elastic constants of nCB

$T_{NI}-T$ °C	5CB			6CB			7CB			8CB		
	$\frac{k_{11}}{k_{22}}$	$\frac{k_{33}}{k_{11}}$	$\frac{k_{33}}{k_{22}}$	$\frac{k_{11}}{k_{22}}$	$\frac{k_{33}}{k_{11}}$	$\frac{k_{33}}{k_{22}}$	$\frac{k_{11}}{k_{22}}$	$\frac{k_{33}}{k_{11}}$	$\frac{k_{33}}{k_{22}}$	$\frac{k_{11}}{k_{22}}$	$\frac{k_{33}}{k_{11}}$	$\frac{k_{33}}{k_{22}}$
1	1.80	1.13	2.03	1.77	1.15	2.04	1.70	1.20	2.03	1.94	0.93	1.81
3	1.85	1.21	2.24	1.85	1.19	2.21	1.81	1.21	2.19	2.10	0.95	2.00
5	1.90	1.25	2.38	1.92	1.21	2.33	1.86	1.23	2.29	2.28	1.07	2.44
7	1.91	1.30	2.47	1.98	1.25	2.47	1.90	1.25	2.39			
9	1.91	1.32	2.53				1.93	1.29	2.48			
11	1.94	1.34	2.60				1.92	1.33	2.54			
13	1.94	1.36	2.64				1.96	1.36	2.67			
15	1.94	1.39	2.70				1.96	1.38	2.71			
17							1.98	1.41	2.78			
19							1.98	1.43	2.83			
21							2.0	1.45	2.90			